

PYROELECTRIC DETECTION OF COHERENT RADIATION ON THE CLARA PHASE 1 BEAMLINE

B. S. Kyle¹, R. B. Appleby¹, T. H. Pacey¹, The University of Manchester, Manchester, UK
 P. H. Williams¹, ASTeC, Daresbury Laboratory (STFC), Daresbury, UK
 J. Wolfenden¹, The University of Liverpool, Liverpool, UK
¹also at The Cockcroft Institute, Daresbury Laboratory, Daresbury, UK

Abstract

The impacts of coherent synchrotron radiation (CSR) and space charge in the bunch compressor section of the CLARA Free Electron Laser (FEL) are expected to be significant, given the relatively high charge and short bunch lengths expected. The General Particle Tracer (GPT) code allows for the modelling of these effects in tandem, presenting an opportunity to more reliably estimate their effects on the CLARA beam. To provide confidence in future studies using GPT, a benchmarking study on the CLARA Phase 1 beamline is presented alongside relevant simulations. This study will make use of pyroelectric detectors to measure the emitted coherent power of the CLARA beam as it passes through a dispersive section whilst varying the chirp imparted on the bunches longitudinal phase space (LPS). Simulations presented demonstrate the viability of such a study, with energies between ~10-100 nJ per pulse expected to be incident upon the detector face.

CLARA

CLARA (Compact Linear Accelerator for Research and Applications) is the UK's FEL test facility located at Daresbury Laboratory. Upon completion of the proposed final phase of installation it will be able to produce 250 pC sub-ps electron bunches of up to 250 MeV, with an expected normalised transverse emittance of $\lesssim 1$ mm mrad [1]. In the main operational modes of CLARA bunches will be compressed in a variable bunch compressor (VBC). Because of the short bunch lengths and relatively high charge in the CLARA beam, CSR emitted in the dipoles of the VBC is expected to have a non-trivial effect on the beam.

The energy redistribution characteristic of CSR can lead to uncontrolled microbunching gain in the bunch if an initial energy or density modulation is present (typically acquired from longitudinal space-charge or shot noise). This modulation typically has a wavenumber different than what is desired for FEL seeding [2]. Furthermore the energy spread and emittance growth associated with CSR has been previously shown to hamper FEL power [3], and so determining the effects of CSR in the CLARA beamline is of importance to the CLARA project as a whole.

The CLARA installation is currently in its first phase [4], which consists of the CLARA injector and a dogleg transfer line to the pre-existing VELA beamline (Figure 1). The

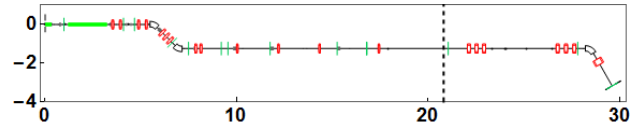


Figure 1: Schematic diagram of the CLARA (Phase 1)/VELA lattice. Accelerating structures are displayed in green, quadrupoles in red, and dipole magnets in white. The dashed line indicates the start of Beam Area 1.

injector itself consists of a 10 Hz 2.5-cell photoinjector gun with accompanying solenoid and bucking coil, and a 2 m long, travelling wave, S-band linac. The VELA beamline is a 23.4 m long transport line which, after passing through a 2 m thick shield wall, is terminated by Beam Area 1 (BA1), a dedicated experimental area.

THEORY

The CSR interaction arises in an ensemble of charges due to the coherent amplification of the individual single-particle synchrotron fields. This amplification only occurs at wavelengths appreciably longer than the bunch length, at which point the radiation is emitted from effectively the same point resulting in a low spread in the emission's phase (Figure 2). As such, the amount of coherent radiated power is strongly dependent upon the bunch length, with shorter bunches radiating more strongly. The spectral density for an ensemble of particles is the product of the single-particle spectral energy density, and a form factor related to the dimensions of the bunch. This spectral density is generally described as [5]

$$\left[\frac{d^2P}{d\Omega d\lambda} \right]_{\text{coh.}} = N(N-1) |F(\underline{k})|^2 \left[\frac{d^2P}{d\Omega d\lambda} \right]_1, \quad (1)$$

where $\frac{d^2P}{d\Omega d\lambda}$ is the spectral density, with the labels coh. and 1 referring to the coherent and the single-particle spectral density respectively, N is the total number of particles in the ensemble, and $F(\underline{k})$ is a 3-dimensional form factor related to the spatial profile of the bunch.

Equation 1 scales as N^2 due to the pairwise nature of the CSR interaction, and can be simplified to a one-dimensional form where only longitudinal effects are considered. This one-dimensional model can be given in terms of the radia-

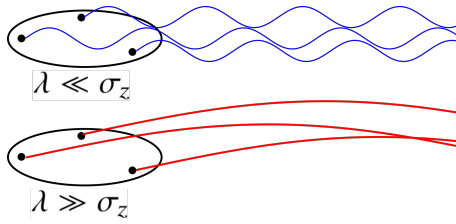


Figure 2: Comparison of short and long wavelength synchrotron emission from an electron bunch.

tion’s frequency rather than wavelength, and for a gaussian longitudinal charge distribution Eq. 1 becomes [6]

$$\left[\frac{d^2P}{d\Omega d\omega} \right]_{\text{coh.}} = N(N-1) e^{-\left(\frac{\omega\sigma_z \cos\theta}{c}\right)^2} \left[\frac{d^2P}{d\Omega d\omega} \right]_1, \quad (2)$$

where $\omega = 2\pi f$, f is the frequency of the radiation, σ_z is the r.m.s bunch length, and θ is the polar angle between the electron bunch’s velocity and the point of observation. This simplification relies on the following criterion (the so-called Derbenev criterion) being met [7]:

$$D = \frac{\sigma_r}{(\rho\sigma_z^2)^{1/3}} \ll 1, \quad (3)$$

where σ_r is the transverse size of the bunch, ρ is the bending radius of the dipole, and σ_z is the bunch length. Many of the CSR models currently implemented in accelerator codes operate in this limit. For an electron bunch in this limit the angular distribution of the coherent radiation is approximately the same as that for a single electron. The radiation emitted by a single electron can be shown to consist of two orthogonal polarisation modes, σ (electric field in bending plane) and π (electric field perpendicular) [8] (Figure 3).

GPT

Simulations presented for the CLARA Phase 1 beamline were carried out in GPT, with space charge calculations carried out using its well-established PIC algorithm [9,10]. The code’s new CSR model is 1-dimensional in that it only calculates the longitudinal component of the CSR field, however it is also able to estimate the effects of the transverse size of the bunch. It employs a method similar to that found in other CSR codes [11], wherein the bunch is longitudinally split into a number of sub-bunches each of which radiates independently. To properly account for radiation emitted at earlier time steps, all particle trajectories are stored in a history manager. A particle’s stored history is deleted when all of the radiation emitted by it has overtaken the entire bunch, also known as the retardation condition.

The fields arising from the CSR interaction are calculated directly from the Liénard-Wiechert fields, resulting in fewer approximations made in the code. Alongside this, GPT’s CSR model is capable of estimating transverse effects upon the longitudinal CSR interaction. Rather than only considering the radiation from a sub-bunch as originating from

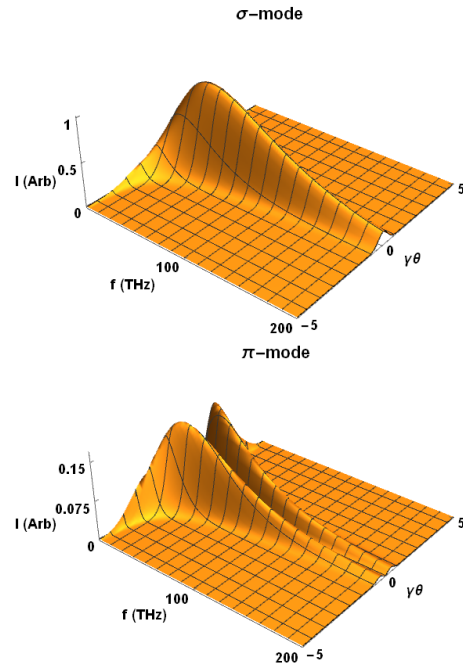


Figure 3: In-plane and perpendicular polarisation of steady-state synchrotron emission from a single 35 MeV electron passing through a uniform dipole of 0.478 m bending radius.

a single axial source point, GPT considers multiple source points offset from the centre of each sub-bunch.

PYROELECTRIC DETECTION OF CSR

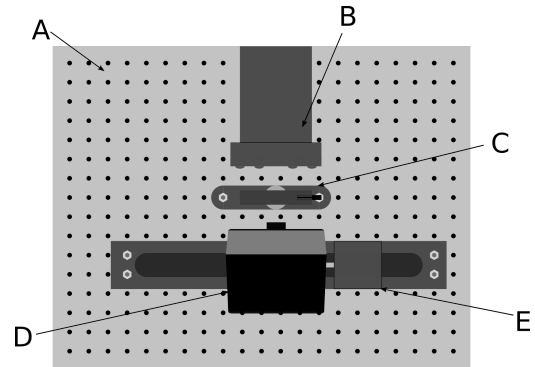


Figure 4: Schematic diagram of the CLARA Phase 1 proposed experimental apparatus: A - optical breadboard, B - quartz window, C - polyethylene polariser (rotatable), D - x-y translation stage, E - gentech-eo PE detector

Previous simulation studies have shown the beam-based effects of CSR (i.e. CSR-induced energy spread) to be too small to measure in the parameter range of CLARA Phase 1 [12]. However, the radiated energy of the bunch is expected to be detectable, with the CSR spectrum expected to peak in the THz region. This motivates the use of pyroelectric (PE) detectors in this proposed experiment, which would be located at the dipole in Beam Area 1 (BA1). There are two ports at this dipole through which the CSR could be detected;

Content from this work may be used under the terms of the CC BY 3.0 licence (© 2018). Any distribution of this work must maintain attribution to the author(s), title of the work, publisher, and DOI.

one currently fitted with a glass window, and the other fitted with a simple metal flange. This experiment would require the replacement of either of these with a quartz window.

The detector system itself will have a relatively simple setup consisting of a PE detector mounted on an x - y translation stage positioned close to the chosen window (Figure 4). This will be accompanied by a THz polariser to allow the horizontal and vertical polarisation modes of the radiation to be characterised. The whole system will be mounted upon an optics breadboard clamped into position. With this setup only the tilt alignment of the camera is important, as the 2-dimensional translation stage facilitates scanning for the radiation signal. While calibration of PE detectors can be carried out at optical wavelengths, the detector's response at various frequencies is unknown and assumed to not be constant. Due to a lack of reliable sources of known energy in the THz region, calibration is currently not possible and absolute values of energy incident on the PE detector cannot be calculated. Instead the incident energy would be measured relative to a nominal case.

SUPPORTING SIMULATIONS

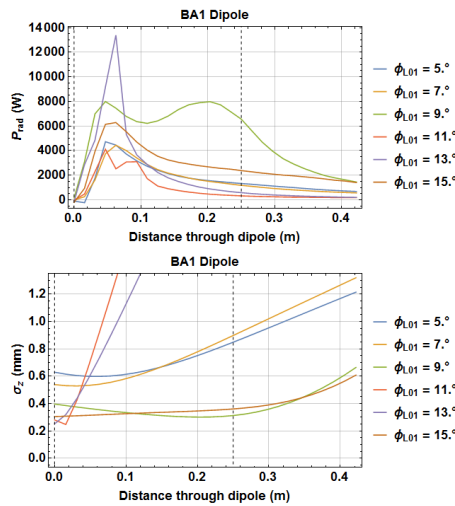


Figure 5: Plots of instantaneous radiated power and r.m.s bunch length for several electron bunches, corresponding to different linac phase offsets, passing through the BA1 dipole in GPT (10^4 macroparticles). Vertical dotted lines show the possible locations from which the radiation can be measured.

GPT simulations were used to calculate the expected radiated power at different bunch lengths. This variation of the bunch length is achieved by varying the off-crest phase of the injector linac (linac-1) which alters the linear chirp in the LPS, which in turn changes the compression factor of the bunch as it passes through the dogleg transfer line to VELA. Simulations presented herein are carried out with a 250 pC electron bunch at a nominal beam energy of ~ 35 MeV

The dogleg transfer line was not designed for compression of electron bunches, and possesses a large second-order

dispersion. This brings about a substantial increase in the beam's transverse emittance, with the normalised emittance (in the bending plane) growing from ~ 2 mm mrad up to ~ 10 mm mrad in the maximal compression case. This poses a challenge while matching the VELA beamline optics, especially considering the presence of drift spaces of up to ~ 3 m long. As such, the beam's transverse profile cannot be kept constant at the entrance to the BA1 dipole with respect to the linac's operating phase (ϕ_{L01}), and this results in the bunch being outside of the Derbenev limit at the dipole entrance for the two most compressed bunches.

Simulations show that despite this large beam emittance, peak powers of up to 6 kW are expected in the BA1 dipole (Figure 5). The output power peaks shortly after the entrance of the dipole, but falls off rapidly as the highly compressed bunches elongate due to reversal of the LPS chirp. An interesting feature is the large amount of radiation emitted towards the start of the dipole, believed to be a transition region effect. However, this occurs a little way into the dipole and is preceded by a fairly low emission rate, which renders the first port (parallel to the incoming beam) unfavourable for the experimental location. A second peak is shown to occur for the $\phi_{L01} = +9^\circ$ case, which corresponds with the bunch length minimum of this two cases. By scanning a range of ϕ_{L01} closer to the on-crest phase, bunches entering the dipole will not yet be maximally compressed. This will slow the rate at which the instantaneous power falls off with respect to distance through the dipole, and has the added advantage of lowering the emittance growth over the dogleg.

The radiated powers correspond to an estimated energy incident on the detector face of between ~ 10 -100 nJ per pulse, which is within the measurable range of the PE detectors. The frequency response of the PE detectors has not been fully characterised, so stated power numbers correspond to radiation emitted over the entire spectrum. However, the majority of this radiation is emitted within a small section of the spectrum where the frequency-response of the detector is expected to be roughly constant. This incident energy ignores any losses caused by optical transport of the radiation.

CONCLUSION

The feasibility of the detection of CSR on CLARA Phase 1 using PE detectors has been demonstrated, with incident energies estimated to be between ~ 0.2 - $0.5 \mu\text{J}$ per pulse. The second port on the BA1 dipole (tangential to half the bend angle) has been shown to be preferable for the location of the experiment, although a different range for the scan of the injector linac's phase offset must be explored to further demonstrate its viability. Further to this, scans of the bunch charge and transverse bunch size should be conducted to demonstrate GPT's accuracy outside of the Derbenev limit.

REFERENCES

- [1] J. A. Clarke *et al.*, CLARA conceptual design report, *JINST*, vol. 9, p. T05001, pp. 16, 2014.
- [2] S. Di Mitri, M. Cornacchia, S. Spanpinati, S. Milton, Suppression of microbunching instability with magnetic bunch length compression in a linac-based free electron laser, *Phys. Rev. ST Accel. Beams*, vol. 13, p. 010702, 2010.
- [3] J. A. G. Akkermans, S. Di Mitri, D. Douglas, I. D. Setija, Compact compressive arc and beam switchyard for energy recovery linac-driven ultraviolet free electron lasers, *Phys. Rev. ST Accel. Beams*, vol. 20, p. 080705, 2017.
- [4] D. Angal-Kalinin *et al.*, Commissioning of front end of CLARA facility at Daresbury Laboratory, in *Proc. IPAC'18*, p. THPMK059, 2018.
- [5] O. Grimm, H. Delsim-Hashemi, J. Rossbach, Transverse electron beam size effect on the bunch profile determination with coherent radiation diagnostics, in *Proc. EPAC'08*, pp. 1113-1115, 2008.
- [6] J. S. Novdick, D. S. Saxon, Suppression of coherent radiation by electrons in a synchrotron, *Phys. Rev.*, vol. 96, no. 1, pp. 180-184, 1954.
- [7] C. C. Hall *et al.*, Measurement and simulation of the impact of coherent synchrotron radiation on the Jefferson Laboratory energy recovery linac electron beam, *Phys. Rev. ST Accel. Beams*, vol. 18, p. 03076, 2015.
- [8] C. Behrens, Detection and spectral measurements of coherent synchrotron radiation at FLASH, *Diploma Thesis, University of Hamburg*, pp. 27-30, 2008.
- [9] S. B. van der Geer, O. J. Luiten, M. J. de Loos, G. Pöplau, U. van Rienen, 3D space-charge model for GPT simulations of high brightness electron bunches, *Institute of Physics Conference Series*, vol. 175, p. 101, 2005.
- [10] G. Pöplau, U. van Rienen, S. B. van der Geer, M. J. de Loos, Multigrid algorithms for the fast calculation of space-charge effects in accelerator design, *IEEE Transactions on magnetics*, vol. 40, p. 714, 2004.
- [11] G. Bassi *et al.*, Overview of CSR codes, *Nucl. Instr. Meth. A*, vol. 557, pp. 189-204, 2006.
- [12] B. S. Kyle *et al.*, CSR and space charge studies for the CLARA phase 1 beamline, in *Proc. IPAC'17*, p. THPAB059, 2017.